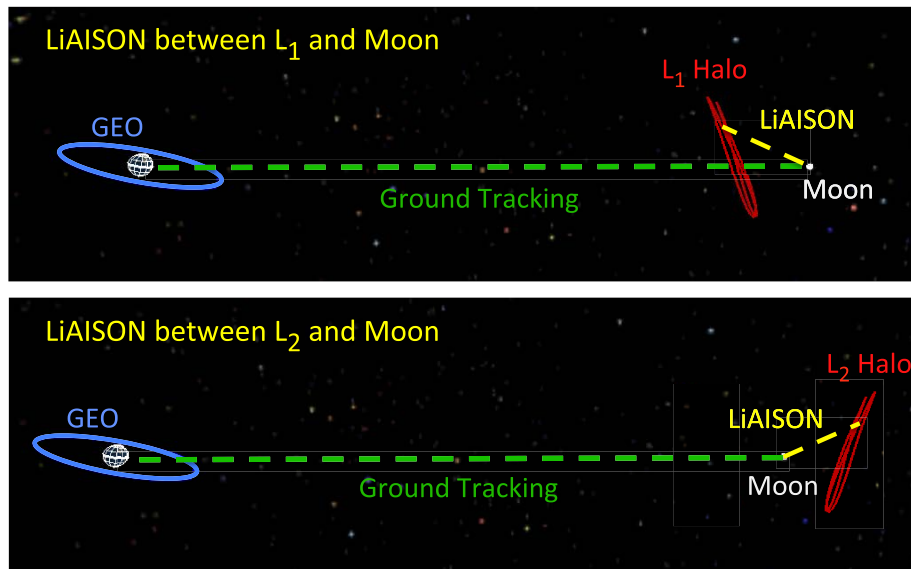


## NAVIGATING A CREWED LUNAR VEHICLE USING LIAISON

Jeffrey S. Parker<sup>\*</sup>, Jason M. Leonard<sup>†</sup>, Kohei Fujimoto<sup>†</sup>,  
Ryan M. McGranaghan<sup>†</sup>, George H. Born<sup>‡</sup> and Rodney L. Anderson<sup>§</sup>

This paper examines the benefits of navigating a crewed vehicle at the Moon using both ground tracking and satellite-to-satellite tracking, where the tracking satellite is stationed in a lunar halo orbit. Linked Autonomous Interplanetary Satellite Orbit Navigation (LiAISON) is a new technique that has been shown to dramatically improve the navigation of lunar satellites, libration orbiters, and Earth orbiting satellites using simple scalar satellite-to-satellite observations, such as range or Doppler. In this paper, LiAISON is applied to the problem of navigating a crewed vehicle in low lunar orbit. It has been found that adding LiAISON observations to a ground navigation solution improves the navigation enough to reduce the number of active ground tracking stations from six to three.



**Figure 1.** The scenarios studied in this paper include a crewed spacecraft in low lunar orbit being tracked by the Deep Space Network from the Earth and from a navigation satellite located in orbit about the Earth-Moon  $L_1$  (top) or  $L_2$  (bottom) libration points.

<sup>\*</sup> Assistant Research Professor, Colorado Center for Astrodynamics Research, University of Colorado, Boulder, CO 80309.

<sup>†</sup> Research Assistant, Colorado Center for Astrodynamics Research, University of Colorado, Boulder, CO 80309.

<sup>‡</sup> Director Emeritus, Colorado Center for Astrodynamics Research, University of Colorado, Boulder, CO 80309.

<sup>§</sup> Member of Technical Staff, Jet Propulsion Laboratory, California Institute of Technology, M/S 301-121, 4800 Oak Grove Dr., Pasadena, CA 91109.

## INTRODUCTION

Recent work has begun measuring the benefits of placing a navigation satellite near the Moon in a libration point orbit (LPO) about either the Earth-Moon  $L_1$  or  $L_2$  point. This satellite may be a dedicated navigation satellite or it may offer satellite-to-satellite tracking (SST) when the opportunity presents itself. This navigation concept is known as LiAISON navigation (Linked Autonomous Interplanetary Satellite Orbit Navigation). Previous work has demonstrated very clearly that LiAISON offers significant benefit to the navigation of satellites virtually anywhere in the Earth-Moon system, including lunar orbits, geostationary orbits, even outbound interplanetary transfers. Further, LiAISON offers a remarkable advantage: it generates *absolute* navigation of any vehicle relative to the Earth and Moon, even without ground observations. It is hypothesized that LiAISON may offer significant benefits and perhaps compelling cost savings if it is applied to assist in the navigation of a crewed vehicle to the Moon, at the Moon, and returning from the Moon. This paper quantifies what improvements LiAISON can offer to the navigation of such a crewed mission in low lunar orbit.

LiAISON navigation has been studied in a wide variety of architectures, including as few as two satellites placed in many combinations of lunar libration orbits such as  $L_1$  and  $L_2$  halo orbits, low lunar orbits, low Earth orbits, geosynchronous orbits, and interplanetary departures.<sup>1-10</sup> Each study has demonstrated that LiAISON can indeed offer accurate satellite navigation even without ground observations. Further, the studies demonstrate that it may be very cost effective to supplement a small amount of ground tracking with a small amount of LiAISON – the geometrical advantage of tracking a satellite from the ground *and* from an LPO are sizable.<sup>8</sup> This illustrates that a dedicated navigation satellite can spend its time tracking multiple customers, reducing the navigation costs of each mission. A sample of the results that LiAISON generates is provided in the next section of this paper.

NASA has been considering new mission concepts for future lunar explorers. One concept is to fly a mission very similar to the Apollo missions: sending humans into low lunar orbit and eventually descending to the surface. Another concept is to send humans on a cruise that flies past the Moon and enters a libration orbit about the Earth-Moon  $L_2$  point. This is considered to be a compelling waypoint mission on the exploration road to Mars. Other options exist as well, such as following a double-lunar swingby or entering an orbit about the Earth-Moon  $L_1$  point on the near side of the Moon.

Each of these lunar mission concepts requires accurate spacecraft navigation in order to perform accurate lunar flybys or to just remain on an  $L_1$  or  $L_2$  orbit. These tight navigation requirements are challenging considering that a crewed vehicle is typically a noisy vehicle; that is, crewed vehicles have historically included a large amount of unmodeled acceleration from outgassing, wastewater dumping, frequent maneuvers, frequent attitude changes, etc. The Apollo ground network compensated for these unmodeled accelerations by tracking the spacecraft with as many as 12 ground stations located around the world. Recent examinations have demonstrated that a similar mission may be tracked with as few as 6 ground stations, provided they are positioned in very beneficial locations.<sup>11</sup>

This paper examines the benefits of supplementing the ground tracking of a crewed mission in low lunar orbit with simple scalar SST generated by a LiAISON satellite located in a halo orbit about  $L_1$  or  $L_2$ . If the LiAISON satellite is designed as a dedicated navigation satellite compatible with the Deep Space Network (DSN), then the crewed vehicle may not even require any hardware modifications. Two proposed navigation architectures are illustrated in Figure 1. It is shown here that the LiAISON tracking data may be used to achieve significant improvements in the navigation accuracy of the crewed vehicle. Alternatively, LiAISON may be used to reduce the number of ground stations from six to three: the same three DSN sites that are currently active and operating. This may offer a means to reduce the operations costs of a crewed mission to the Moon.

## BACKGROUND

### Lunar Exploration

*History* There have been around 80 missions to have flown to the Moon, including robotic missions conducted by several nations and including the crewed Apollo missions. Many of these missions simply flew past the Moon, perhaps en route to other destinations such as WMAP, AsiaSat-3, and STEREO; others impacted the Moon, such as Luna 2, Ranger 4, and LCROSS. Many missions have entered lunar orbit, a few have landed, including the famous Apollo landings, and several returned from the Moon back to the Earth. Each of these missions has required a significant tracking campaign to ensure that its navigation requirements are met. The navigation requirements have steadily gotten tighter and it is expected that they will continue to get more demanding in the future. All missions to date have relied upon radiometric tracking from antennas such as those in the Deep Space Network, though it is not unprecedented to suggest using a halo orbiter for communication relay.<sup>12-14</sup> A communication relay could easily provide navigation services as well; this research continues to discover new benefits to a navigation satellite located in such an orbit.

*The Lunar Gravity Field* The gravity field of the Moon caused significant errors in early missions, since it was not well known at that time. The Apollo missions reported that mass concentrations, referred to as "Masscons", beneath the lunar surface significantly perturbed the spacecraft's orbit. For instance, the initial orbit of the Apollo 8 mission had a periapse altitude of 110.6 km and an apoapse altitude of 112.4 km.<sup>15</sup> After only 24 hours in orbit, the orbit's periapse altitude had dropped to 108.5 km and its apoapse altitude had risen to 117.8 km. While some of this change was predicted, this was a larger variation than expected.

Lunar Prospector helped reduce the navigation errors caused by the Moon's gravity field. It mapped the Moon from January 1998 through July 31, 1999 and developed a gravity field that was modeled by a spherical harmonic expansion of degree and order 150: the LP150q gravity field.<sup>16</sup> The uncertainty in this gravity field is far lower on the near side of the Moon than on the far side, since Lunar Prospector was not tracked on the far side. Missions such as the Lunar Reconnaissance Orbiter and GRAIL have used the LP150q gravity field and have achieved position uncertainties better than 100 meters ( $1\sigma$ ).<sup>17,18</sup>

The GRAIL mission has generated several complex maps of the full lunar gravity field – near side and far side – that may be modeled by spherical harmonic expansions with degree and order greater than 420.<sup>19</sup> Higher expansions are being developed, but have not yet been released as of February 2013. Even the 420x420 map makes the Moon's gravity field the best known gravity field in the solar system; it should dramatically reduce the contributions of gravitational errors to all current and future missions at the Moon.

The current work uses experiences from Apollo to quantify the navigation uncertainty caused by human activities aboard a spacecraft. It should be recognized that the Apollo missions also experienced large navigation uncertainties caused by errors in the lunar gravity model and it is not clear which source of errors caused the reported navigation errors. Gravity modeling errors should be all but removed from future human exploration.

*Operating a Satellite in a Libration Orbit* The two ARTEMIS spacecraft demonstrated successful spacecraft operations in LPOs as they traversed trajectories about both the Earth-Moon  $L_1$  and  $L_2$  points ( $LL_1$  and  $LL_2$ , respectively) from late 2010 through mid-2011.<sup>20,21</sup> They did so using a significant amount of ground-based tracking from the Deep Space Network, the Universal Space Network (USN) and the Berkeley Ground Station (BGS) located at the University of California at Berkeley.<sup>22,23</sup> Navigating these trajectories requires care since they are unstable trajectories: a perturbation in an orbital state will double in magnitude every day or two. The navigation data included range and Doppler observations from DSN and USN antennae and Doppler observations from BGS. The nominal strategy involved collecting 3.5 hours of DSN tracking data every other day, alternating between stations in the northern and southern hemispheres, two 45-minute tracks of BGS data every day, and one 30-minute track of USN data per week.<sup>23</sup> Navigators were able to determine each of the satellites' states to within approximately 100 meters in position and approximately 1 mm/s in velocity at any time.<sup>22</sup> Each spacecraft performed station keeping maneuvers approximately once per week while in libration orbits, requiring approximately 0.5 m/s per month of  $\Delta V$ .

A benefit of LiAISON is that all navigation operations in an LPO may be performed autonomously, as

demonstrated by Hill, et al.,<sup>3</sup> removing the tracking requirements and maneuver planning demands from the ground. Of course, any mission to perform LiAISON first will be shadowed by ground navigators.

*Proposed Exploration* It has been proposed to send humans on missions to various locations near the Moon, including libration orbits about the lunar Lagrange points, as well as low lunar orbits and the lunar surface. It is expected that the errors in the navigation system due to the Moon's gravity will be much smaller than they were for the Apollo missions. However, humans have never flown on a libration orbit before, which being unstable, may make the navigation more challenging than it was for the Apollo missions. Further, if NASA or another space entity is interested in establishing a permanent presence at the Moon, then a robust navigation architecture will be required. LiAISON may indeed be one link in this architecture much like GPS is a significant link in navigation near the Earth and on its surface.

This paper studies the case of supporting a crewed mission in low lunar orbit, since many analogs may be drawn between this system and the Apollo experiences. Concurrent studies are examining the scenarios where LiAISON is introduced to the navigation system for a crewed vehicle performing a trans-lunar cruise and traversing an orbit about LL<sub>2</sub>.<sup>10</sup>

### **Unfortunate Lack of Acceleration Knowledge (FLAK)**

Crewed vehicles such as the Apollo vehicles and the proposed Orion vehicle typically perform frequent activities that cannot be fully modeled in a navigation simulation, but which perturb the spacecraft's trajectory. These activities and their corresponding disturbances may include any of the following:<sup>11,24</sup>

- Attitude adjustments via reaction control engines that are not perfectly coupled, which result in small translational accelerations.
- Angular momentum desaturation maneuvers that are performed to reduce the angular speeds of any momentum wheels onboard the vehicle. These maneuvers are also performed via the reaction control system and result in small translational accelerations.
- Wastewater venting, which results in a translational acceleration that may be performed in a particular direction, but the timing and magnitude of which is often not well predicted.
- Venting of gasses, such as CO<sub>2</sub>, which also may be performed in a known direction, but the timing and magnitude of acceleration is not well predicted.
- Heat rejection via sublimation of water and associated venting.
- Unmodeled attitude changes that result in changes to radiation pressure on the spacecraft, which results in a small change in the radiation pressure acceleration vector. The change is not necessarily in the Sun-spacecraft line due to potential changes in the radiation reflection angles.

The combination of all of these potential disturbances has come to be known as FLAK (**un**fortunate **l**ack of **a**cceleration **k**nowledge).<sup>10, 11, 24</sup>

At present, the models for all future human vehicles are not mature enough to properly model the uncertainties caused by each of these potential acceleration sources. To remain consistent with literature,<sup>11</sup> FLAK has been modeled in this examination as a source of uncertainty that grows in a spherically-symmetric fashion, yielding a position uncertainty of approximately 500 meters (1- $\sigma$ ) every hour while in a low lunar orbit.

The magnitude of the total FLAK acceleration drops while the crew sleeps, presumably because wastewater dumps cease and other systems onboard the spacecraft settle into a more steady state. The literature models sleep periods as having 10% of the total FLAK acceleration as during the waking periods.<sup>11</sup>

## Ground Networks

The ground network that was constructed to support the Apollo missions involved as many as a dozen land-based and sea-based tracking sites located around the Earth, illustrated in Figure 2. The tracking data collected by this Manned Space Flight Network included two-way and three-way range and Doppler measurements. The network included good East-West baselines between ground stations as well as some good North-South baselines.

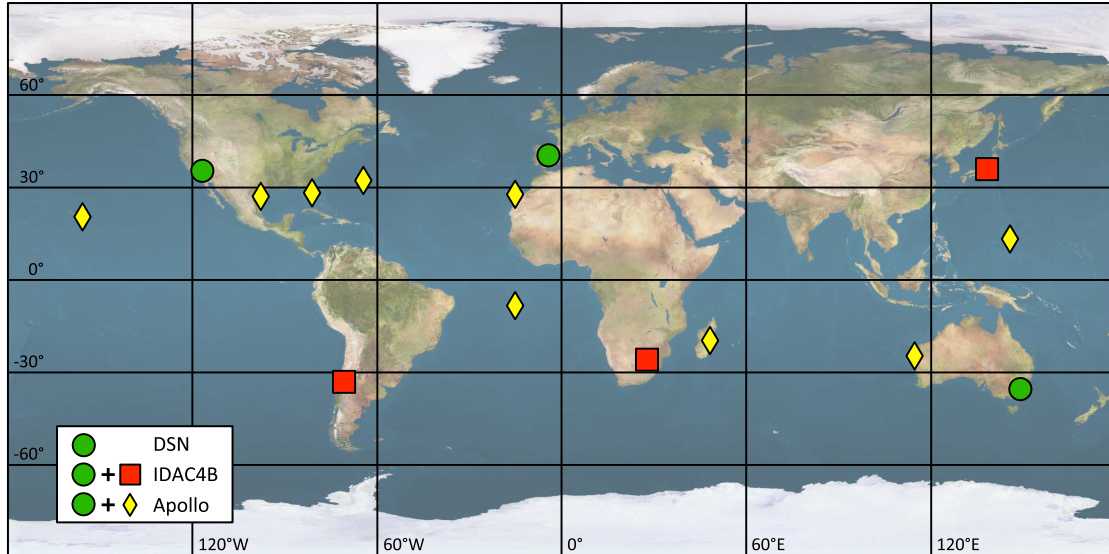


**Figure 2. The locations of tracking stations in three different ground networks, including the Deep Space Network (circles), the IDAC4B (circles and squares), and the Apollo ground network (circles and diamonds).**

After Apollo 17, the network condensed to become the Deep Space Network, containing three primary sites located in Goldstone, California; Madrid, Spain; and Canberra, Australia. This system has been sufficient to support a large number of deep space probes, but recent studies have demonstrated that it may not be sufficient for the navigation needs of a modern crewed exploration to the Moon.<sup>11</sup>

A previous study led by the Constellation program identified three locations that could supplement the three DSN sites and provide substantial North-South baselines as well as strong East-West baselines: enough to be sufficient for supporting modern lunar exploration. These sites were identified in the *integrated design and analysis* (IDAC) 4B analysis cycle, hence the name "IDAC4B". The three new sites include stations located in Santiago, Chile, in Hartebeesthoek, South Africa, and in Usuda, Japan, as illustrated in Figure 2. Notice that each of the three DSN sites has a counterpart in the opposite hemisphere. The three new IDAC4B sites would likely be receive-only stations, cooperating with the DSN sites as three-way receiving stations. The locations of each of the ground stations in the DSN and IDAC4B networks used in the current simulations is presented in Table 1. These are approximate locations of each station and do not correspond with any particular antenna.

For the purpose of the simulations presented here, each of these stations has a 10 degree elevation mask. The IDAC4B sites are indeed receive-only and perform three-way tracking with whichever DSN site is in view. If multiple DSN sites are in view of the spacecraft, only one site tracks the spacecraft: Goldstone is prioritized if it is available, followed by Madrid and then Canberra. Each of the IDAC4B receive-only stations are assigned to provide complementary services with one DSN site; for the purpose of this study, Santiago and Goldstone work together, Hartebeesthoek and Madrid work together, and Usuda and Canberra work together. Hence, only one DSN site and at most one IDAC4B receive-only station are active at any

**Table 1. The latitude, longitude, and altitude of each of the three DSN sites and the remaining three IDAC4B sites used in this research, relative to a spherical Earth with a radius of 6378.14 km. Longitudes are presented in Eastward coordinates.**

| Station        | Latitude | Longitude | Altitude |
|----------------|----------|-----------|----------|
| Goldstone      | 35.247°  | 243.205°  | 1.071 km |
| Madrid         | 40.427°  | 4.251°    | 0.835 km |
| Canberra       | -35.398° | 148.982°  | 0.692 km |
| Santiago       | -33.450° | 289.333°  | 0.731 km |
| Hartebeesthoek | -25.890° | 27.687°   | 1.414 km |
| Usuda          | 36.139°  | 138.363°  | 1.456 km |

given time.

### LiAISON Navigation

LiAISON navigation takes advantage of particular circumstances to generate *absolute* orbit navigation using only relative satellite-to-satellite tracking data.<sup>1-10</sup> Ordinarily, SST data provides relative information about the orientation of the orbits of both vehicles: at best nine out of twelve degrees of freedom in the system.<sup>25</sup> This conclusion depends on an implied assumption that the vehicles are both orbiting a body, such as the Earth, in a near-conic orbit and that the system is not sensitive enough to discern any perturbations in the force field. LiAISON, however, operates when one or both of the satellites involved is indeed sensitive to asymmetries in the force field. Certainly an obvious example of this is the case of SST between an Earth orbiter and a lunar orbiter: one cannot simply rotate that system around the Earth's center and achieve trajectories that generate equivalent range or range-rate time profiles. Similarly, one cannot just rotate an LPO about the Earth or Moon: it is anchored to both the Earth and the Moon in order to exist.

Two particular cases have been thoroughly studied: Hill et al. simulated a practical navigation mission at the Moon involving one or more libration orbiters and a robotic low lunar orbiter;<sup>3,5</sup> Parker et al., and Leonard et al., studied scenarios where a satellite in a libration orbit about the Earth-Moon  $L_1$  point tracked a GEO satellite.<sup>7,8</sup> Both scenarios demonstrated how the relative tracking data resulted in absolute navigation knowledge using realistic errors and models.

Figure 3 provides an illustration of the basic concept that Hill et al. studied in depth.<sup>3,5</sup> The simulation involves as many realistic components as possible, including high-fidelity dynamical models, realistic maneuver execution models, realistic observation schedules, etc. The two satellites track each other using relative range and range-rate observations, including measurement errors. The results indicate that the low lunar orbiter's state may be estimated to within 10 meters in position and 1 cm/s in velocity over time and the  $LL_2$  halo orbiter's state may be estimated to within 100 meters in position and 1 mm/s in velocity over time ( $1\sigma$ ). No ground observations were included in any lunar LiAISON simulation.

Hill et al. demonstrated that a constellation of two or more satellites may be used to autonomously navigate several receptive satellites simultaneously near the Moon. This is an interesting result because the system requires no ground observations at all. We suggest an alternative that requires only one satellite: a single satellite in an LPO may be able to provide a navigation beacon, much like GPS, to navigate any number of receptive satellites simultaneously at the Moon, in orbit about the Earth, or elsewhere in the system, as long as the LPO satellite is able to access some of the tracking data from those receptive satellites and/or from ground tracking. If each satellite involved has a very accurate clock, such as the Deep Space Atomic Clock currently being developed at JPL,<sup>26</sup> then there would be no need to establish two-way communication. This reduces the complexity of applied LiAISON.

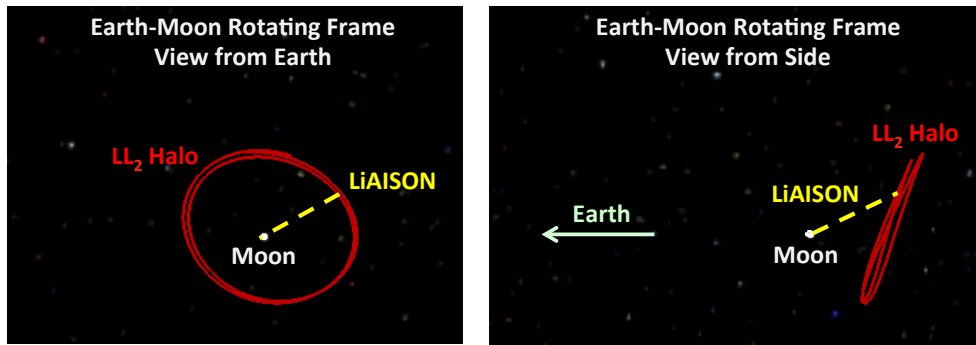


**Figure 3.** An illustration of LiAISON applied to the case of one satellite in a halo orbit about  $LL_2$  and a satellite in a 100 km polar lunar orbit performing autonomous mutual navigation.

## MISSION CONCEPT

The mission considered here is one where a crewed vehicle is in orbit about the Moon, being tracked by a combination of ground tracking and satellite-to-satellite tracking. The ground tracking may be from the three primary DSN sites or from all six IDAC4B ground sites. The satellite-to-satellite tracking is from a lunar libration orbiter in orbit about either the Earth-Moon  $L_1$  point or  $L_2$  point. The lunar libration orbiter may be optionally tracked by the DSN as well. Each of these configurations will be considered.

## Orbits

NASA has indicated an interest in the lunar poles and eventually landing near a pole. The crewed vehicle in these studies supports a landing at any location: it is in a circular lunar orbit with an altitude of 100 km, an inclination of 90 degrees, and a longitude of ascending node of 30 degrees in the IAU Moon Fixed coordinate frame at an epoch of January 1, 2020 00:00:00 ET (Ephemeris Time). The International Astronomical Union (IAU) developed this lunar fixed coordinate frame such that its  $z$ -axis is aligned with the right-handed spin-axis of the Moon and a set of polynomials defines the pole direction over time relative to the International Celestial Reference Frame.<sup>27</sup> For brevity, it is sufficient to state that the  $z$ -axis points in the direction of the Moon's spin-axis and the  $0^\circ$  longitude points roughly toward the Earth over time.

The lunar libration orbiter is placed in a halo orbit about either the Earth-Moon  $L_1$  or  $L_2$  point, depending on the scenario. The  $L_1$  halo orbit is slightly more geometrically advantageous as a tracking vehicle to support the crewed vehicle along a direct Earth-Moon transfer;<sup>10</sup> the  $L_2$  halo orbit is beneficial because it can track the vehicle when the crew is behind the Moon. Figure 3 illustrates the  $L_2$  option; the  $L_1$  orbit is very similar but on the near side of the Moon, relative to Earth. Table 2 summarizes the orbital parameters of the halo orbits used here; more information about constructing these orbits is provided in literature.<sup>7,28,29</sup>

**Table 2.** The parameters of the  $L_1$  and  $L_2$  halo orbits simulated here. For simplicity, the same parameter set is used in the algorithms to generate both types of orbits.

| Parameter | Value                | Comments                             |
|-----------|----------------------|--------------------------------------|
| $A_z$     | 35,500 km            | The $z$ -axis amplitude              |
| $\phi$    | $0^\circ$            | The initial phase angle of the orbit |
| $t_{ref}$ | 1/1/2020 00:00:00 ET | The reference epoch, ephemeris time  |

One significant advantage of a libration orbit, such as a halo orbit, is that the navigation satellite can be placed into that orbit using very little fuel by implementing a low-energy transfer.<sup>7,28</sup> These transfers take

advantage of the Sun’s gravity over the course of 3–4 months to give the spacecraft the necessary energy to just slip into orbit without requiring any sizable orbit insertion maneuver. In fact, Parker shows that no fuel at all is required except for trajectory corrections.<sup>28,30</sup>

### Tracking Data

Simple range and range-rate tracking data is simulated between the DSN and each vehicle near the Moon, as well as between the lunar libration orbiter and the crewed low lunar orbiter. There are many sources of errors in each of these links, including atmospheric influences, clock errors, path-length errors, etc. In this study, the errors are simplified into two parameters per link: a systematic bias that is added to each and every observation between each transmitter and receiver and a random white-noise process that changes with every observation. The bias is randomly selected from a Gaussian distribution with zero mean and some given standard deviation. The same bias is then applied to each observation for a given link. In reality this bias may change from one pass to another between the DSN and a spacecraft; this bias may also drift during a pass. This level of fidelity will be applied to future simulations, as well as light time corrections, as minor as those effects may be. It is assumed that each link establishes two-way (or three-way for the IDAC4B sites) communication, reducing any clock errors. The resulting models for range and range-rate between antennae 1 and 2 are:

$$\rho_{12} = \sqrt{(\mathbf{r}_1 - \mathbf{r}_2) \cdot (\mathbf{r}_1 - \mathbf{r}_2)} + \rho_{12}^{bias} + \rho_{12}^{noise} \quad (1)$$

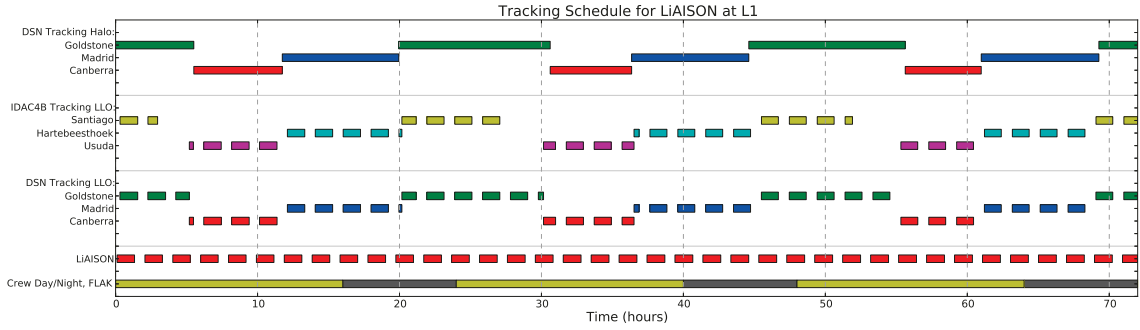
$$\dot{\rho}_{12} = \frac{(\mathbf{r}_1 - \mathbf{r}_2) \cdot (\dot{\mathbf{r}}_1 - \dot{\mathbf{r}}_2)}{\rho_{12}} + \dot{\rho}_{12}^{bias} + \dot{\rho}_{12}^{noise} \quad (2)$$

Table 3 summarizes the bias and white noise placed on each of tracking link in these scenarios.

**Table 3. The parameters used to define the errors in the tracking data. The bias added to each link and the white noise added to each observation are drawn from Gaussian distributions with zero mean and the given standard deviations. The  $L_1$  and  $L_2$  orbiters have the same tracking data characteristics, indicated by *LPO*.**

| Tracking Link                 | Bias 1- $\sigma$ | White Noise 1- $\sigma$ | Comments                                     |
|-------------------------------|------------------|-------------------------|--|
| LPO - LLO 2-way range         | 3 m              | 1 m                     | LiAISON range SST                            |
| LPO - LLO 2-way range-rate    | 1 mm/s           | 1 mm/s                  | LiAISON range-rate SST                       |
| DSN - LPO 2-way range         | 30 m             | 10 m                    | DSN ground tracking of the halo orbiter      |
| DSN - LPO 2-way range-rate    | 1 mm/s           | 0.5 mm/s                |  |
| DSN - LLO 2-way range         | 30 m             | 10 m                    | DSN ground tracking of the crewed vehicle    |
| DSN - LLO 2-way range-rate    | 1 mm/s           | 0.5 mm/s                |  |
| IDAC4B - LLO 3-way range      | 30 m             | 10 m                    | IDAC4B ground tracking of the crewed vehicle |
| IDAC4B - LLO 3-way range-rate | 1 mm/s           | 0.5 mm/s                |  |

Figure 4 illustrates the timeline of observations that are simulated for a crewed vehicle in low lunar orbit and a libration orbiter at  $L_1$ . The timeline for a scenario that places the libration orbiter at  $L_2$  is very similar: the significant exception is that the LiAISON tracking data is available on the far side of the Moon rather than the near side. Figure 5 illustrates a compressed version that highlights the differences between the  $L_1$  and  $L_2$  architectures. Of course, not all scenarios process all observations. As mentioned earlier, there may be overlaps where two DSN stations and/or two IDAC4B stations can view either of the vehicles, but the simulations process data from only one DSN station and one IDAC4B station at a time. It is assumed that each DSN site has antennas available to track both the halo orbiter and the crewed vehicle, if needed. It is assumed that the IDAC4B sites never track the halo orbiter. Looking carefully at the figures, one can see that that the  $L_1$  satellite can see the crewed vehicle further behind the Moon than the ground stations can, but that the crewed vehicle still has periods of time when nothing can track it. Whereas the  $L_2$  satellite fills in the ground tracking gaps nicely.



**Figure 4.** An illustration of the schedule of tracking observations for the case of an  $L_1$  halo orbiter. Not all observations are used in all scenarios.

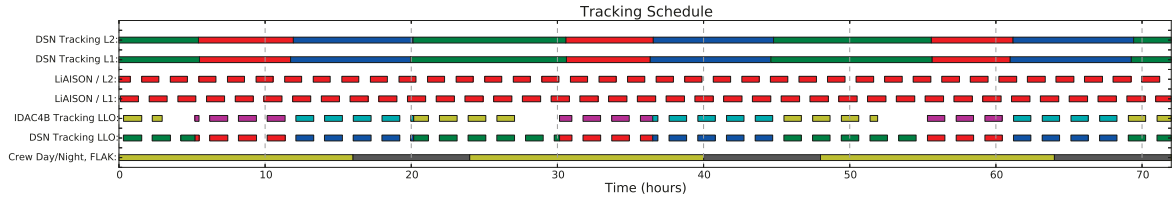


**Figure 5.** A compressed timeline, illustrating when each tracking option is in view.

## Models

The dynamical model used includes the force of gravity of the Earth, Moon, Sun, and all planets in the solar system, where each body’s positions have been modeled using JPL’s Planetary and Lunar Ephemerides DE405.<sup>31</sup> The lunar gravity field includes a  $20 \times 20$  spherical harmonic expansion using the LP150q gravity field.<sup>16</sup> Each vehicle has also been assigned an area-to-mass ratio of 0.01 and exposed to solar radiation pressure at all times except while in shadow of the Moon. Neither vehicle ever enters the Earth’s shadow. The solar radiation pressure is modeled as a flat-plate with a nominal  $C_R$  value of 1.0.

## Covariance Studies

It is early to perform a full navigation simulation of a crewed vehicle at the Moon since FLAK is not well defined yet. However, it is straightforward to perform a covariance analysis of several architectures and compare them for complexity and performance. It is assumed in this study that FLAK dominates the dynamical errors for the crewed vehicle, but it is not clear how it will actually act on the spacecraft. Thus, the covariance study is a good step to take at this time.

The navigation simulations set up the vehicle trajectories and process each observation using a Kalman filter.<sup>7,32</sup> The process begins with an *a priori* covariance matrix, representing the initial uncertainty in the state of the system; as observations are processed this covariance matrix may shrink or grow, depending on the amount of information present in the observations, the certainty of the observations, and the amount of time between observations.

The state vector  $\mathbf{X}$  used in the analyses performed here includes a simple set of 12 parameters: the position and velocity of both the libration orbiter and the crewed lunar vehicle:

$$\mathbf{X} = [ \mathbf{R}_{LPO}^T, \mathbf{V}_{LPO}^T, \mathbf{R}_{Crew}^T, \mathbf{V}_{Crew}^T ]^T,$$

where the subscript  $LPO$  corresponds to the libration point orbiter and the subscript  $Crew$  corresponds to

the crewed vehicle.

The *a priori* covariance,  $\bar{P}_0$ , used in each study, unless otherwise noted, is tight for the libration point orbiter and loose for the crewed vehicle. It is presumed that the libration orbiter has been tracked prior to the onset of LiAISON. This is not necessary, but it reduces the time needed for the navigation to converge on a steady state uncertainty level. The *a priori* covariance is a  $12 \times 12$  diagonal matrix with the following values on the diagonal:

$$\bar{P}_0 = \text{Diag} \left( \sigma_{x,LPO}^2, \sigma_{y,LPO}^2, \sigma_{z,LPO}^2, \sigma_{\dot{x},LPO}^2, \sigma_{\dot{y},LPO}^2, \sigma_{\dot{z},LPO}^2, \dots, \sigma_{x,Crew}^2, \sigma_{y,Crew}^2, \sigma_{z,Crew}^2, \sigma_{\dot{x},Crew}^2, \sigma_{\dot{y},Crew}^2, \sigma_{\dot{z},Crew}^2 \right),$$

where each uncertainty has been set to the following:

- 100 meter  $1-\sigma$  uncertainty on each position component of the libration point orbiter;
- 1 m/s  $1-\sigma$  uncertainty on each velocity component of the libration point orbiter;
- 10 km  $1-\sigma$  uncertainty on each position component of the crewed vehicle;
- 10 m/s  $1-\sigma$  uncertainty on each velocity component of the crewed vehicle.

The observation covariance matrix,  $R$ , remains constant throughout each simulation and represents the amount of noise placed on the observations. It is assumed that each observation data type is uncorrelated and independent. Hence,  $R$  is equal to a diagonal matrix with the following values on the diagonal, as applicable to the scenario being studied:

$$R = \text{Diag} \left( \sigma_{\rho,LiAISON}^2, \sigma_{\dot{\rho},LiAISON}^2, \sigma_{\rho,DSNi-LPO}^2, \sigma_{\dot{\rho},DSNi-LPO}^2, \dots, \sigma_{\rho,DSNi-Crew}^2, \sigma_{\dot{\rho},DSNi-Crew}^2, \sigma_{\rho,IDAC4Bi-Crew}^2, \sigma_{\dot{\rho},IDAC4Bi-Crew}^2 \right),$$

where each uncertainty has been set to the level of noise on the corresponding observation (not including the bias), as summarized in Table 3. In a scenario that includes range and range-rate between all possible links, the  $R$  matrix is  $20 \times 20$  in size, corresponding to range and range-rate between the two vehicles, between the three DSN stations and the LPO, between the three DSN stations and the crewed vehicle, and between the three IDAC4B receive-only stations and the crewed vehicle. Most scenarios involve fewer observation types.

State noise compensation is used to inflate the covariance to prevent filter saturation and to accommodate for uncertainties in the dynamical model, including FLAK. Process noise is injected into the equations of motion as follows:<sup>32</sup>

$$\dot{\mathbf{X}}(t) = \mathbf{f}(t, \mathbf{X}(t), \mathbf{u}(t)), \quad (3)$$

where  $\mathbf{u}(t)$  is a zero-mean Gaussian white noise vector. The process noise transition matrix is constructed as a matrix of partial derivatives:

$$\Gamma(t_i, t_j) = \frac{\partial \mathbf{X}(t_i)}{\partial \mathbf{u}(t_j)}. \quad (4)$$

The process noise transition matrix maps the uncertainty introduced by process noise, i.e., unmodeled acceleration, to the appropriate state parameters over time.

The basic Kalman filter maps the state's associated variance-covariance matrix at some time  $t_j$ ,  $P(t_j)$ , to the epoch of the next observation  $t_i$  using a linearized state transition matrix,  $\Phi(t_i, t_j)$ :

$$\bar{P}(t_i) = \Phi(t_i, t_j)P(t_j)\Phi(t_i, t_j)^T. \quad (5)$$

More details may be found in literature.<sup>7,32</sup> The filter then processes the observation(s) at  $t_i$  generating  $P(t_i)$ , which is smaller than  $\bar{P}(t_i)$  since the observation provides additional information about the state.

Process noise is introduced during the time update to account for the unmodeled accelerations that add uncertainty to the state during the passage of time. Hence, the covariance matrix at time  $t_i$  prior to processing

the observations at  $t_i$  may be modified to include some *a priori* process noise covariance at that time,  $\bar{Q}(t_i)$ . Equation 5 is updated to include process noise as follows:

$$\bar{P}(t_i) = \Phi(t_i, t_j)P(t_j)\Phi(t_i, t_j)^T + \bar{Q}(t_i). \quad (6)$$

The process noise covariance matrix is mapped through time much like the variance-covariance matrix:

$$\bar{Q}(t_i) = \Gamma(t_i, t_j)Q(t_j)\Gamma(t_i, t_j)^T, \quad (7)$$

where  $Q(t_j)$  is typically expressed as a diagonal matrix with specified  $\sigma^2$  values along the diagonal.

Process noise is added to compensate for unmodeled accelerations in both the crewed vehicle and the libration orbiter. Of course FLAK is a large unmodeled acceleration and dominates the unmodeled accelerations of the crewed vehicle; the libration orbiter on the other hand is likely to be a relatively well-modeled spacecraft in a very benign environment. The  $Q(t_j)$  matrix to account for the unmodeled accelerations experienced by the libration orbiter is quite small: it is a  $3 \times 3$  diagonal matrix with diagonal elements of  $\sigma^2 = (5 \times 10^{-15} \text{ km/s}^2)^2$ . The process noise transition matrix,  $\Gamma(t_i, t_j)$ , is constructed simply to account for the passage of time since the previous observation,  $\Delta t = t_i - t_j$ , linearly approximated as:

$$\Gamma(t_i, t_j) = \begin{bmatrix} \Delta t^2/2 \times \mathbf{I}_{3 \times 3} \\ \Delta t/2 \times \mathbf{I}_{3 \times 3} \end{bmatrix}. \quad (8)$$

This formulation assumes that the dynamics vary trivially from one observation to the next, which is a good assumption in this study. The state noise compensation for FLAK is mechanically precisely the same, but the magnitude is far greater. The experiences in the Apollo program indicated that unmodeled accelerations contributed to approximately 500 meters of position error over the course of one hour while in low lunar orbit. Empirical testing estimates that the  $Q(t_j)$  matrix should have diagonal elements of  $\sigma^2 \approx (1.195 \times 10^{-5} \text{ m/s}^2)^2$  in order to permit the position uncertainty to grow by about 500 meters in an hour while in low lunar orbit. The magnitude of FLAK drops by an order of magnitude during sleep periods: roughly eight hours of the day.

### Cramér-Rao Lower Bound

The Cramér-Rao Lower Bound (CRLB) or Cramér-Rao inequality may be computed to measure the lower bound on the uncertainty that a particular unbiased estimator may achieve if it is optimal.<sup>33-36</sup> If an orbit determination filter is achieving an uncertainty in its estimates near the CRLB, then no further tuning of the filter is necessary. Conversely, if one's results are far worse than the CRLB, then it may be useful to continue tuning the filter to achieve less uncertainty in the results.

If  $P$  is the estimation error covariance matrix that corresponds to any unbiased estimator of the unknown state parameters, and  $P^*$  is the CRLB, then one may state:

$$P \geq P^* \equiv J^{-1},$$

where  $J$  is the Fisher information matrix. One computes  $P^*$  simply using a Kalman filter, linearized about the truth trajectory rather than the best estimate of the trajectory. The covariance studies performed here are therefore generating the CRLB for the navigation simulations of these scenarios. In the presence of process noise, the Fisher information matrix may be computed at any time using the following recursive relationship, where the subscripts represent the corresponding matrices at that time:

$$J_i = Q_j^{-1} + \tilde{H}_i^T R_i^{-1} \tilde{H}_i - Q_j^{-1} \Phi(t_i, t_j) (J_j + \Phi(t_i, t_j) Q_j^{-1} \Phi(t_i, t_j)^T)^{-1} \Phi(t_i, t_j)^T Q_j^{-1}, \quad (9)$$

where  $\tilde{H}$  is an observation mapping matrix.<sup>7,32</sup>

## SIMULATIONS

### LiAISON-only

The first simulation studied here is a validation of two assumptions: (1) that a small *a priori* covariance may be used for the lunar libration orbiter and (2) that LiAISON does indeed achieve reasonable navigation uncertainties without any ground tracking. A scenario has been simulated using an L<sub>1</sub> halo orbiter and the crewed lunar orbiter described above, but with a large *a priori* covariance matrix, such that the position  $1\sigma$  values have been set to 100,000 km and the velocity  $1\sigma$  values have been set to 1000 km/s. Figure 6 illustrates how the position uncertainties of both vehicles drop over time just processing corrupted SST data. The uncertainty of the crewed vehicle reaches a steady-state after only 2–3 days of tracking; the halo orbiter hasn't reached a steady-state level of uncertainty after 12 days, but it is certainly within reasonable navigation accuracy after a week.

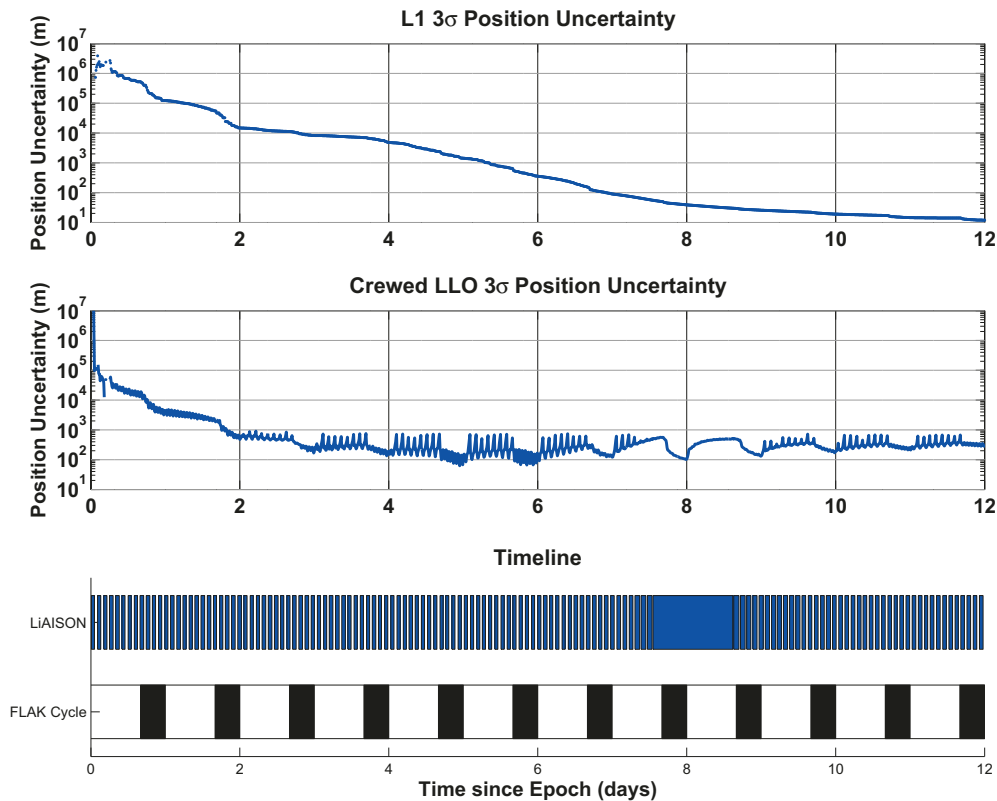


**Figure 6. The position  $3\sigma$  uncertainty of the halo orbiter (top) and the crewed lunar orbiter (middle) while processing LiAISON-only observation data using very large *a priori* covariances. The FLAK time profile and availability of LiAISON data is shown at the bottom.**

It is interesting to see in Figure 6 how the level of FLAK influences the uncertainty of the crewed vehicle but not the halo orbiter. It is also interesting to see the navigation uncertainty as the low lunar orbiter's plane precesses about the Moon, relative to the halo orbiter. Around day 8, the crewed vehicle's orbital plane is nearly face-on, which reduces the variations in the range and range-rate time profiles and consequently raises the uncertainty in the crewed vehicle's state; but the lack of occultations helps to balance the loss of geometrical information. The navigation results for an L<sub>2</sub> halo orbiter are very similar.

This simulation demonstrates that LiAISON may be used by itself to achieve acceptable levels of uncertainty and it is a fair assumption to begin the halo orbiter with a tight covariance in order to accelerate the time it takes to reach steady-state. It is reasonable to expect that ground tracking will be used to prepare the halo orbiter prior to supporting a crewed vehicle.

### Ground-only

The second simulation validates that the ground-only tracking of both vehicles also achieves reasonable navigation accuracies with very large *a priori* uncertainty. Figure 7 illustrates the results of the simulation where the three primary DSN sites track both vehicles and LiAISON is not included. One sees that the navigation reaches steady-state slightly quicker than the LiAISON-only simulation. It is also worth noting that the navigation accuracy of the crewed vehicle is worse when its orbit is face-on, around the 10th day of the simulation, despite the lack of occultations.

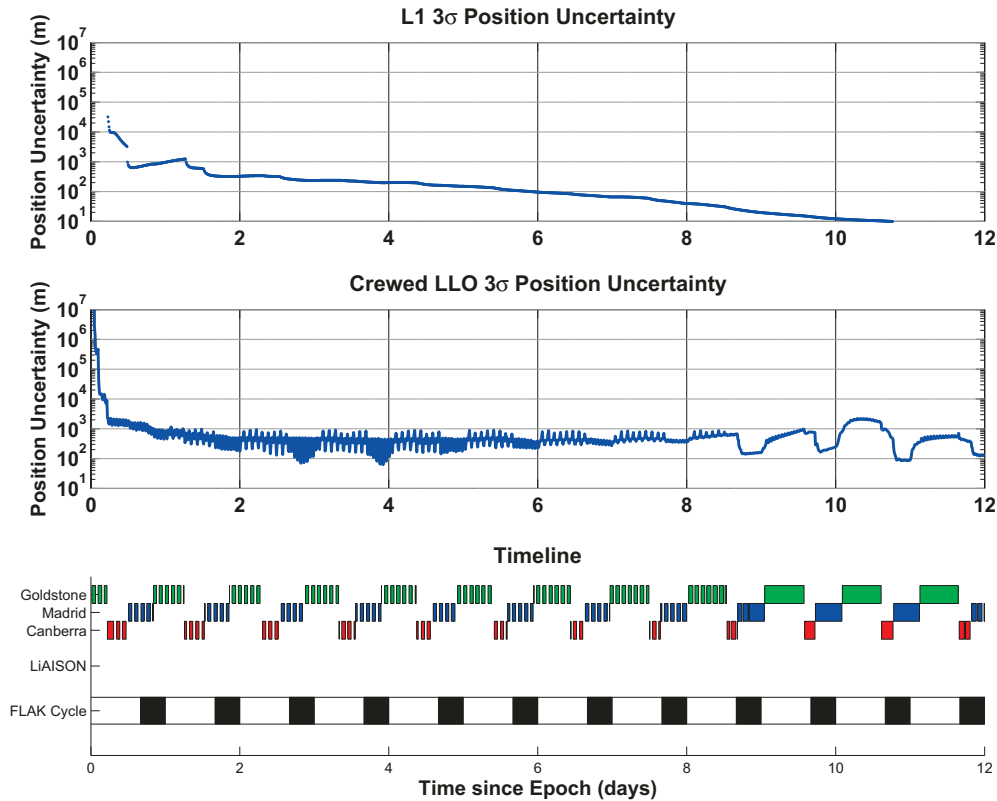


**Figure 7. The position  $3\sigma$  uncertainty of the halo orbiter (top) and the crewed lunar orbiter (middle) while processing ground-only observation data from the three DSN sites using very large *a priori* covariances. The FLAK time profile and availability of DSN tracking data is shown at the bottom.**

Now that it has been shown that a steady-state navigation performance is achievable from very large *a priori* uncertainties, each remaining simulation will use the smaller  $\bar{P}_0$  presented above.

### DSN+LiAISON

The simulation considered here, prior to delving into a large trade study, is to consider the differences between LiAISON tracking from an L<sub>1</sub> halo vs. an L<sub>2</sub> halo orbiter. The geometrical benefits are very similar

when either LiAISON observations are used by themselves. But the  $L_2$  orbiter offers a significant benefit over the  $L_1$  orbiter when used in concert with ground-based tracking because the tracking data is not occulted when ground tracking is and vice versa. That is, the  $L_2$  LiAISON data achieves a more steady navigation performance over time. Figure 8 illustrates this over four days of tracking, processing observations from the three DSN stations and a libration orbiter, illustrating the difference between  $L_1$  and  $L_2$  tracking, respectively. Table 4 summarizes the navigation performance for these two configurations. Three performance measures have been considered: (1) the mean  $3\sigma$  position uncertainty of the crewed vehicle, which does capture some information about the benefits of the night-time FLAK cycle, (2) the 99th percentile  $3\sigma$  position uncertainty, and (3) the maximum (100th percentile)  $3\sigma$  position uncertainty observed in the simulation. Each of these metrics is computed using data from 3–7 days after the simulation’s start, giving time for the simulation to reach a steady-state. The third metric is useful, but it is sensitive to the time steps taken in the simulation and the arbitrary timing as the spacecraft comes out of lunar occultation. It is clear that the  $L_2$  halo orbiter performs far better in general than the  $L_1$  halo orbiter, considering each of these metrics. It is also clear that the navigation performance is more consistent between near-side passages and far-side passages since the 99th and 100th percentiles of the position uncertainties fall further for the  $L_2$  case than the mean position uncertainty.

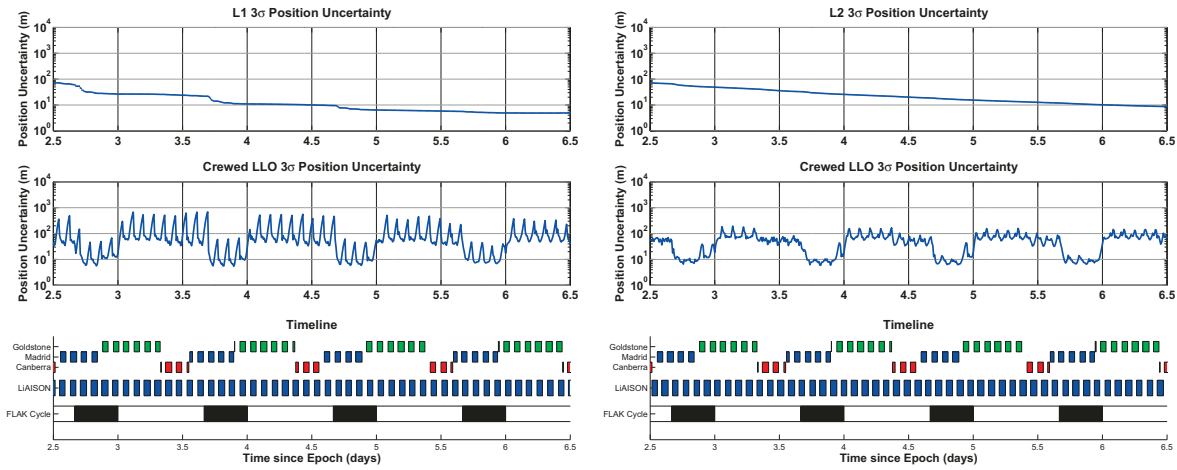


**Figure 8.** The position  $3\sigma$  uncertainty of the halo orbiter (top) and the crewed lunar orbiter (middle) while processing DSN and  $L_1$  (left) /  $L_2$  (right) LiAISON tracking data.

**Table 4.** The  $3\sigma$  position uncertainties observed in a system that includes the crewed low lunar orbiter and a lunar libration orbiter, being tracked by the three DSN stations and LiAISON.

| <b>LiAISON with <math>L_1</math></b> |                            |                           |                           |
|--------------------------------------|----------------------------|---------------------------|---------------------------|
| Vehicle                              | Mean $3\sigma$ uncertainty | 99% $3\sigma$ uncertainty | Max $3\sigma$ uncertainty |
| $L_1$ Halo                           | 10.3 meters                | 26.5 meters               | 26.5 meters               |
| Crewed LLO                           | 92.6 meters                | 540.9 meters              | 687.1 meters              |
| <b>LiAISON with <math>L_2</math></b> |                            |                           |                           |
| Vehicle                              | Mean $3\sigma$ uncertainty | 99% $3\sigma$ uncertainty | Max $3\sigma$ uncertainty |
| $L_2$ Halo                           | 19.5 meters                | 47.7 meters               | 48.6 meters               |
| Crewed LLO                           | 53.7 meters                | 158.5 meters              | 192.1 meters              |

## Simulation Survey

The three simulations presented so far have illustrated how the system achieves a steady state performance even with large initial uncertainties and only SST data. There are numerous variations in the architecture that will be considered in a survey presented here. The simulations studied here vary whether or not LiAISON is included, if it is performed from  $L_1$  or  $L_2$ , which ground stations are included, whether or not they track the halo orbiter as well as the crewed vehicle, and whether or not to include range, range-rate, or both types of radiometric tracking data in each link. Of course with this many variations only a few cost functions will be presented.

Each architecture has been simulated for 12 days, giving time for the low lunar orbit's geometry to vary relative to the ground and the halo orbits. The simulations typically reach a steady state in only one or two days; to give a little margin, the steady state navigation metrics are computed using data between day 3 and day 12 of the simulation. It is most interesting to observe the variations in the mean and 99th percentile of the position uncertainty, since they capture information about the trends and extremes observed in the architecture without being quite as sensitive to outliers as the 100th percentile.

Table 5 summarizes the architectures studied here and the resulting navigation performance of each. Figure 9 graphically presents both the mean and the 99th percentile of the crewed vehicle's  $3\sigma$  position uncertainty for each of the scenarios. Many conclusions may be drawn. First, it is not surprising that the scenarios with more tracking data perform better than those with fewer data. It is also not surprising that each scenario performs better with both range and range-rate data types than with just one. However, there are some scenarios where the range-only tracking performed better than the range-rate-only tracking, e.g., the LiAISON-only scenarios; in other scenarios the range-rate-only cases outperformed the range-only cases, e.g., the DSN-only scenarios.

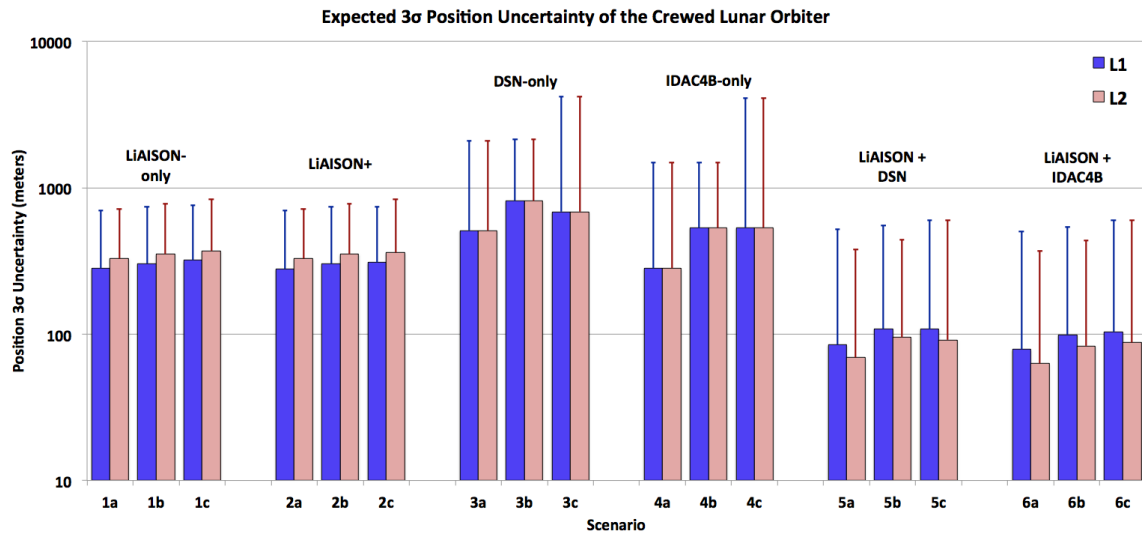


**Figure 9.** The  $3\sigma$  position uncertainty of the crewed lunar orbiter for a variety of scenarios. The main shaded bars illustrate the mean  $3\sigma$  position uncertainties over time for each scenario and the thin error bar extensions on top illustrate the 99th percentile of the  $3\sigma$  position uncertainties over time. The scenarios are defined in Table 5.

The difference between each version of Scenario 1 and the corresponding version of Scenario 2 is that the halo orbiter is tracked by the DSN as well as by LiAISON in Scenario 2. The crewed vehicle is tracked via LiAISON only in both cases. The results indicate that the DSN tracking barely improves the performance: the halo orbiter's navigation uncertainty improves by just a few kilometers in position. This is a strong

**Table 5. The scenarios studied in this survey, including their definitions and resulting performance.**

| Scenario | Halo Orbit     | LiAISON included | Halo           | Crew           | Crew              | Range Data | Range-Rate Data | 3 $\sigma$ Pos Uncertainty of LLO (km) |        |        |
|----------|----------------|------------------|----------------|----------------|-------------------|------------|-----------------|--|--------|--------|
|          |                |                  | Tracked by DSN | Tracked by DSN | Tracked by IDAC4B |            |                 | Mean                                   | 99%    | Max    |
| 1a-1     | L <sub>1</sub> | 1                | 0              | 0              | 0                 | 1          | 1               | 281.6                                  | 698.5  | 742.7  |
| 1a-2     | L <sub>2</sub> | 1                | 0              | 0              | 0                 | 1          | 1               | 329.5                                  | 712.7  | 832.9  |
| 1b-1     | L <sub>1</sub> | 1                | 0              | 0              | 0                 | 1          | 0               | 303.9                                  | 744.2  | 787.1  |
| 1b-2     | L <sub>2</sub> | 1                | 0              | 0              | 0                 | 1          | 0               | 353.7                                  | 776.4  | 844.0  |
| 1c-1     | L <sub>1</sub> | 1                | 0              | 0              | 0                 | 0          | 1               | 319.6                                  | 757.3  | 897.6  |
| 1c-2     | L <sub>2</sub> | 1                | 0              | 0              | 0                 | 0          | 1               | 371.5                                  | 831.4  | 979.8  |
| 2a-1     | L <sub>1</sub> | 1                | 1              | 0              | 0                 | 1          | 1               | 279.9                                  | 696.8  | 741.3  |
| 2a-2     | L <sub>2</sub> | 1                | 1              | 0              | 0                 | 1          | 1               | 328.5                                  | 712.4  | 832.5  |
| 2b-1     | L <sub>1</sub> | 1                | 1              | 0              | 0                 | 1          | 0               | 301.3                                  | 743.9  | 786.5  |
| 2b-2     | L <sub>2</sub> | 1                | 1              | 0              | 0                 | 1          | 0               | 351.8                                  | 774.4  | 842.7  |
| 2c-1     | L <sub>1</sub> | 1                | 1              | 0              | 0                 | 0          | 1               | 310.0                                  | 745.4  | 895.9  |
| 2c-2     | L <sub>2</sub> | 1                | 1              | 0              | 0                 | 0          | 1               | 361.0                                  | 831.0  | 979.4  |
| 3a-1     | L <sub>1</sub> | 0                | 0              | 1              | 0                 | 1          | 1               | 511.4                                  | 2087.9 | 2223.3 |
| 3a-2     | L <sub>2</sub> | 0                | 0              | 1              | 0                 | 1          | 1               | 511.4                                  | 2087.9 | 2223.3 |
| 3b-1     | L <sub>1</sub> | 0                | 0              | 1              | 0                 | 1          | 0               | 812.1                                  | 2156.0 | 2276.4 |
| 3b-2     | L <sub>2</sub> | 0                | 0              | 1              | 0                 | 1          | 0               | 812.1                                  | 2156.0 | 2276.4 |
| 3c-1     | L <sub>1</sub> | 0                | 0              | 1              | 0                 | 0          | 1               | 687.2                                  | 4209.0 | 6528.5 |
| 3c-2     | L <sub>2</sub> | 0                | 0              | 1              | 0                 | 0          | 1               | 687.2                                  | 4209.0 | 6528.5 |
| 4a-1     | L <sub>1</sub> | 0                | 0              | 1              | 1                 | 1          | 1               | 282.7                                  | 1494.4 | 1653.4 |
| 4a-2     | L <sub>2</sub> | 0                | 0              | 1              | 1                 | 1          | 1               | 282.7                                  | 1494.4 | 1653.4 |
| 4b-1     | L <sub>1</sub> | 0                | 0              | 1              | 1                 | 1          | 0               | 532.2                                  | 1495.0 | 1653.8 |
| 4b-2     | L <sub>2</sub> | 0                | 0              | 1              | 1                 | 1          | 0               | 532.2                                  | 1495.0 | 1653.8 |
| 4c-1     | L <sub>1</sub> | 0                | 0              | 1              | 1                 | 0          | 1               | 535.9                                  | 4116.6 | 6180.8 |
| 4c-2     | L <sub>2</sub> | 0                | 0              | 1              | 1                 | 0          | 1               | 535.9                                  | 4116.6 | 6180.8 |
| 5a-1     | L <sub>1</sub> | 1                | 1              | 1              | 0                 | 1          | 1               | 84.7                                   | 518.5  | 687.1  |
| 5a-2     | L <sub>2</sub> | 1                | 1              | 1              | 0                 | 1          | 1               | 69.4                                   | 379.4  | 636.8  |
| 5b-1     | L <sub>1</sub> | 1                | 1              | 1              | 0                 | 1          | 0               | 109.0                                  | 553.8  | 716.1  |
| 5b-2     | L <sub>2</sub> | 1                | 1              | 1              | 0                 | 1          | 0               | 94.9                                   | 442.1  | 641.8  |
| 5c-1     | L <sub>1</sub> | 1                | 1              | 1              | 0                 | 0          | 1               | 108.4                                  | 602.4  | 855.7  |
| 5c-2     | L <sub>2</sub> | 1                | 1              | 1              | 0                 | 0          | 1               | 91.5                                   | 603.7  | 723.4  |
| 6a-1     | L <sub>1</sub> | 1                | 1              | 1              | 1                 | 1          | 1               | 78.7                                   | 501.0  | 650.7  |
| 6a-2     | L <sub>2</sub> | 1                | 1              | 1              | 1                 | 1          | 1               | 63.0                                   | 372.1  | 601.7  |
| 6b-1     | L <sub>1</sub> | 1                | 1              | 1              | 1                 | 1          | 0               | 99.2                                   | 541.9  | 710.9  |
| 6b-2     | L <sub>2</sub> | 1                | 1              | 1              | 1                 | 1          | 0               | 83.2                                   | 435.9  | 606.5  |
| 6c-1     | L <sub>1</sub> | 1                | 1              | 1              | 1                 | 0          | 1               | 104.0                                  | 602.3  | 855.7  |
| 6c-2     | L <sub>2</sub> | 1                | 1              | 1              | 1                 | 0          | 1               | 87.7                                   | 603.7  | 723.4  |

argument for not spending more time tracking the halo orbiter than is necessary. Of course in a real mission the halo orbiter will be tracked from time to time, but one of the benefits of the LiAISON architecture is that its navigation *can* be entirely autonomous.

The results presented here illustrate that continuous LiAISON-only tracking performs roughly on par with the IDAC4B ground system and quite a bit better than the DSN-only ground system. Combining LiAISON with ground tracking immensely improves the navigation (Scenarios 5 and 6 from Table 5 and Figure 9). If one has the three DSN stations prepared for the mission and has to choose between adding three more to create the IDAC4B network or adding a halo orbiter, the halo orbiter is far better from a navigation performance perspective.

### Varying FLAK

The results of the navigation simulations produced here certainly depend on the level of FLAK. Figure 10 illustrates how the 3 $\sigma$  position uncertainty changes as the level of FLAK varies for Scenario 5a-1 (LiAISON

and DSN tracking both vehicles using range and range-rate; no IDAC4B). One can see that the effect is very linear: if FLAK is multiplied by some factor then the resulting navigation uncertainty will also be scaled by that factor. This is a useful result because FLAK is not well modeled yet; as long as FLAK may be modeled as a spherically symmetric growth of the state estimate covariance matrix, the results presented in this paper apply to any reasonable level of FLAK via a scaling factor.

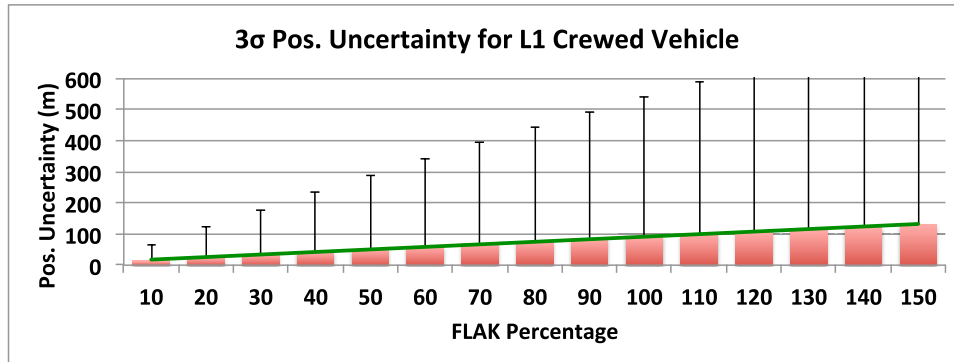


Figure 10. The effect of changing the level of FLAK in the simulation.

## CONCLUSIONS

This paper has presented several navigation simulations of a crewed vehicle in a low polar lunar orbit, where it is being tracked by a combination of DSN ground stations, IDAC4B ground stations, and/or satellite-to-satellite tracking via LiAISON (Linked, Autonomous, Interplanetary Satellite Orbit Navigation). It has been assumed that without any tracking data, the position uncertainty of the crewed vehicle will rise by approximately 500 meters over the course of an hour due to unmodeled accelerations known as FLAK. The results presented here may be linearly scaled with the level of FLAK provided that FLAK is applied to the estimated covariance matrix in a spherically symmetric way.

The results presented here demonstrate that LiAISON alone can provide enough information to track both the crewed vehicle and the lunar navigation satellite to within a few hundred meters relative to an inertial frame, using only range and range-rate data. This agrees with LiAISON results in the literature.

The mean RSS position uncertainty ( $3\sigma$ ) for the crewed vehicle in a DSN-only tracking scenario is approximately 500 – 800 meters, using the assumptions in this paper and depending on which tracking data type is used. By adding three more ground stations and constructing the IDAC4B constellation (see Figure 2), the position uncertainty drops to approximately 280 – 530 meters ( $3\sigma$  RSS); almost half of the DSN-only scenario. If instead a lunar navigation satellite is added and LiAISON tracking is introduced, then the navigation uncertainty drops further to 85 – 109 meters ( $3\sigma$  RSS). If all data available are processed, including the DSN, IDAC4B, and LiAISON, then the position uncertainty drops even further to 63 – 104 meters ( $3\sigma$  RSS).

A navigation satellite in a lunar halo orbit provides significant navigation benefits. As NASA works to establish a permanent presence near the Moon, the navigation benefits of such a satellite will become more important.

## Acknowledgements

The authors would like to thank Roby Wilson and Matt Abrahamson at the Jet Propulsion Laboratory for their valuable feedback during the editing of this paper. The research presented in this paper has been partially carried out at the Jet Propulsion Laboratory, California Institute of Technology, under a contract with the National Aeronautics and Space Administration. Government sponsorship acknowledged.

## REFERENCES

- [1] K. Hill, M. W. Lo, and G. H. Born, "Linked, Autonomous, Interplanetary Satellite Orbit Navigation (LiAISON)," *Proceedings of the AAS/AIAA Astrodynamics Specialist Conference held 7-11 August 2005, South Lake Tahoe, California, Paper AAS 05-399* (B. G. Williams, L. A. D'Amario, K. C. Howell, and F. R. Hoots, eds.), Vol. 123 of *Advances in Astronautical Sciences*, San Diego, CA, AAS/AIAA, Univelt Inc., 2006.
- [2] K. Hill, G. H. Born, and M. W. Lo, "Linked, Autonomous, Interplanetary Satellite Orbit Navigation (LiAISON) in Lunar Halo Orbits," *Proceedings of the AAS/AIAA Astrodynamics Specialist Conference held 7-11 August 2005, South Lake Tahoe, California, Paper AAS 05-400* (B. G. Williams, L. A. D'Amario, K. C. Howell, and F. R. Hoots, eds.), Vol. 123 of *Advances in Astronautical Sciences*, San Diego, CA, AAS/AIAA, Univelt Inc., 2006.
- [3] K. Hill, J. S. Parker, G. H. Born, and N. Demandante, "A Lunar L2 Navigation, Communication, and Gravity Mission," *AIAA/AAS Astrodynamics Specialist Conference*, No. AIAA 2006-6662, Keystone, Colorado, AIAA/AAS, August 2006.
- [4] K. Hill and G. H. Born, "Autonomous Interplanetary Orbit Determination Using Satellite-to-Satellite Tracking," *AIAA Journal of Guidance, Control, and Dynamics*, Vol. 30, May–June 2007.
- [5] K. Hill, *Autonomous Navigation in Libration Point Orbits*. PhD thesis, University of Colorado, Boulder, Colorado, 2007.
- [6] J. S. Parker, R. L. Anderson, G. H. Born, and K. Fujimoto, "Linked Autonomous Interplanetary Satellite Orbit Navigation (LiAISON) Between Geosynchronous and Lunar Halo Orbits," Tech. Rep. D-72688, Jet Propulsion Laboratory, California Institute of Technology, 4800 Oak Grove Dr., Pasadena, California, 2012.
- [7] J. S. Parker, R. L. Anderson, G. H. Born, K. Fujimoto, J. M. Leonard, and R. M. McGranaghan, "Navigation Between Geosynchronous and Lunar L1 Orbiters," *AIAA/AAS Astrodynamics Specialist Conference*, No. AIAA-2012-4878, Minneapolis, Minnesota, AIAA/AAS, 13–16 August 2012.
- [8] J. M. Leonard, R. M. McGranaghan, K. Fujimoto, G. H. Born, J. S. Parker, and R. L. Anderson, "LiAISON-Supplemented Navigation for Geosynchronous and Lunar L1 Orbiters," *AIAA/AAS Astrodynamics Specialist Conference*, No. AIAA-2012-4664, Minneapolis, Minnesota, AIAA/AAS, 13–16 August 2012.
- [9] K. Fujimoto, J. M. Leonard, R. M. McGranaghan, J. S. Parker, R. L. Anderson, and G. H. Born, "Simulating the LiAISON Navigation Concept in a GEO + Earth-Moon Halo Constellation," *Proceedings of the 23rd International Symposium on Space Flight Dynamics (ISSFD)*, Pasadena, CA, 29 Oct – 2 Nov 2012.
- [10] J. M. Leonard, J. S. Parker, R. L. Anderson, R. M. McGranaghan, K. Fujimoto, and G. H. Born, "Supporting Crewed Lunar Exploration with LiAISON Navigation," *2013 Guidance, Navigation, and Control Conference*, No. 13-053, Breckenridge, Colorado, AAS, 1–6 February 2013.
- [11] T. A. Ely, M. Heyne, and J. E. Riedel, "Altair Navigation Performance During Translunar Cruise, Lunar Orbit, Descent, and Landing," *Journal of Spacecraft and Rockets*, Vol. 49, March–April 2012, pp. 295–317.
- [12] A. C. Clarke, *Interplanetary Flight*. London: Temple Press Books Ltd., 1950.
- [13] R. W. Farquhar, "Station-Keeping in the Vicinity of Collinear Libration Points with an Application to a Lunar Communications Problem," *Space Flight Mechanics*, Vol. 11 of *Science and Technology Series*, pp. 519–535, New York: American Astronautical Society, 1966.
- [14] R. W. Farquhar, "Lunar Communications with Libration-Point Satellites," *Journal of Spacecraft and Rockets*, Vol. 4, No. 10, 1967, pp. 1383–1384.
- [15] R. W. Orloff, *Apollo by the Numbers: A Statistical Reference (The Second Mission: Testing the CSM in Lunar Orbit)*. Washington, DC: NASA History Division, Office of Policy and Plans.
- [16] A. S. Konopliv, S. W. Asmar, E. Carranza, W. L. Sjogren, and D. N. Yuan, "Recent Gravity Models as a Result of the Lunar Prospector Mission," *International Journal of Solar System Studies*, Vol. 150, No. 1, 2001, pp. 1–18.
- [17] E. Mazarico, D. D. Rowlands, G. A. Neumann, D. E. Smith, M. H. Torrence, F. G. Lemoine, and M. T. Zuber, "Orbit Determination of the Lunar Reconnaissance Orbiter," *Journal of Geodesy*, Vol. 86, March 2012, pp. 193–207.
- [18] T.-H. You, P. Antreasian, S. Broschart, K. Criddle, E. Higa, D. Jefferson, E. Lau, S. Mohan, M. Ryne, and M. Keck, "Gravity Recovery and Interior Laboratory Mission (GRAIL) Orbit Determination," *Proceedings of the 23rd International Symposium on Space Flight Dynamics (ISSFD)*, Pasadena, CA, 29 Oct – 2 Nov 2012.
- [19] F. G. Lemoine, S. J. Goossens, T. J. Sabaka, J. B. Nicholas, E. Mazarico, D. D. Rowlands, B. D. Loomis, D. S. Chinn, D. S. Caprette, J. J. McCarthy, G. A. Neumann, M. T. Zuber, and D. E. Smith, "High Degree and Order Gravity Fields of the Moon Derived from GRAIL Data," *American Geophysical Union Meeting*, San Francisco, CA, 3–7 December 2012.
- [20] S. B. Broschart, M. J. Chung, S. J. Hatch, J. H. Ma, T. H. Sweetser, S. S. Weinstein-Weiss, and V. Angelopoulos, "Preliminary Trajectory Design for the ARTEMIS Lunar Mission," *Proceedings of*

- the AAS/AIAA Astrodynamics Specialist Conference held 9-13 August 2009, Pittsburgh, Pennsylvania, Paper AAS 09-382 (A. V. Rao, T. A. Lovell, F. K. Chan, and L. A. Cangahuala, eds.), Vol. 134 of *Advances in Astronautical Sciences*, San Diego, CA, AAS/AIAA, Univelt Inc., 2009.
- [21] M. Woodard, D. Folta, and D. Woodfork, "ARTEMIS: The First Mission to the Lunar Libration Orbits," *21st International Symposium on Space Flight Dynamics*, Toulouse, France, Centre National d'Études Spatiales, September 28 – October 2, 2009.
- [22] D. Folta, M. Woodard, and D. Cosgrove, "Stationkeeping of the First Earth-Moon Libration Orbiters: The ARTEMIS Mission," *Proceedings of the AAS/AIAA Astrodynamics Specialist Conference held 31 July–4 Aug 2011, Girdwood, Alaska, Paper AAS 11-515* (H. Schaub, B. C. Gunter, R. P. Russell, and W. T. Cerven, eds.), Vol. 142 of *Advances in Astronautical Sciences*, San Diego, CA, AAS/AIAA, Univelt Inc., 2012.
- [23] M. Woodard, D. Cosgrove, P. Morinelli, J. Marchese, B. Owens, and D. Folta, "Orbit Determination of Spacecraft in Earth-Moon L1 and L2 Libration Point Orbits," *Proceedings of the AAS/AIAA Astrodynamics Specialist Conference held July 31 to August 4, 2011, in Girdwood, Alaska, Paper AAS 11-514* (H. Schaub, B. C. Gunter, R. P. Russell, and W. T. Cerven, eds.), Vol. 142 of *Advances in Astronautical Sciences*, San Diego, CA, AAS, Univelt Inc., 2012.
- [24] J. Getchius, "CEV Flight Dynamics Team Technical Brief," Tech. Rep. FltDyn-CEV-09-94, On-Orbit GNC Section; Science, Engineering, and Analytical Support Dept., The Engineering and Science Contract Group (ESCG) segment of Jacobs Technology, 30 June 2009.
- [25] Y. Liu and L. Liu, "Orbit Determination Using Satellite-to-Satellite Tracking Data," *Chinese Journal of Astronomy and Astrophysics*, Vol. 1, No. 3, 2001, pp. 281–286.
- [26] T. A. Ely, T. Koch, D. Kuang, K. Lee, D. Murphy, J. Prestage, R. Tjoelker, and J. Seubert, "The Deep Space Atomic Clock Mission," *Proceedings of the 23rd International Symposium on Space Flight Dynamics (ISSFD)*, Pasadena, CA, 29 Oct – 2 Nov 2012.
- [27] B. A. Archinal, M. F. A'Hearn, E. Bowell, A. Conrad, G. J. Consolmagno, R. Courtin, T. Fukushima, D. Hestroffer, J. L. Hilton, G. A. Krasinsky, G. Neumann, J. Oberst, P. K. Seidelmann, P. Stooke, D. J. Tholen, P. C. Thomas, and I. P. Williams, "Report of the IAU Working Group on Cartographic Coordinates and Rotational Elements: 2009," *Celestial Mechanics and Dynamical Astronomy*, Vol. 109, 2011, pp. 101–135.
- [28] J. S. Parker, *Low-Energy Ballistic Lunar Transfers*. PhD thesis, University of Colorado, Boulder, Colorado, 2007.
- [29] D. L. Richardson, "Analytical Construction of Periodic Orbits about the Collinear Points," *Celestial Mechanics*, Vol. 22, 1980, pp. 241–253.
- [30] J. S. Parker, "Targeting Low-Energy Ballistic Lunar Transfers," *Journal of the Astronautical Sciences*, Vol. 58, July–September 2011, pp. 311–334.
- [31] E. M. Standish, "JPL Planetary and Lunar Ephemerides, DE405/LE405," Tech. Rep. IOM 312.F-98-048, Jet Propulsion Laboratory, California Institute of Technology, August 1998.
- [32] B. D. Tapley, B. E. Schutz, and G. H. Born, *Statistical Orbit Determination*. Burlington, MA: Elsevier Academic Press, 2004.
- [33] H. Cramér, *Mathematical Methods of Statistics*. Princeton, New Jersey: Princeton University Press, 1946.
- [34] C. R. Rao, "Information and the Accuracy Attainable in the Estimation of Statistical Parameters," *Bulletin of the Calcutta Mathematical Society*, Vol. 37, 1945, pp. 81–89.
- [35] C. R. Rao, *Selected Papers of C. R. Rao*. New York: Wiley, 1994.
- [36] J. H. Taylor, "The Cramér-Rao Estimation Error Lower Bound Computation for Deterministic Nonlinear Systems," *IEEE Transactions on Automatic Control*, Vol. AC-24, No. 2, 1979, pp. 343–344.